Mullite-Based Ceramics from Mining Waste

Subjects: Mining & Mineral Processing

Contributor: Maximina Romero

Mullite ($3Al_2O_3 \cdot 2SiO_2$) is an aluminosilicate characterized by excellent physical properties, which makes it an important ceramic material. In this way, ceramics based on mullite find applications in different technological fields as refractory material (metallurgy, glass, ceramics, etc.), matrix in composite materials for high temperature applications, substrate in multilayer packaging, protective coatings, components of turbine engines, windows transparent to infrared radiation, etc. However, mullite is scarce in nature so it has to be manufactured through different synthesis methods, such as sintering, melting-crystallization or through a sol-gel route.

Keywords: mullite ; clay-based ceramics ; mining waste ; sterile ; tailings ; iron and aluminum waste ; boron ; molybdenum and lithium waste ; coal gangue ; kaolin waste ; ornamental rock waste

1. Introduction

Nowadays, mining is a critical industry for global economic and social development, and it will continue to be the main resources provider in the immediate future [1]. However, just as there have been great technological advances in mining techniques that allow a larger recovery of minerals and therefore a continuous growth of world production, the impoverishment of deposits in terms of the grade, which requires larger scale, more complex and depth excavations, has an even higher impact on a major generation of waste. Figure 1 shows the evolution of world production of minerals in the 2009–2018 decade [2], and Figure 2 shows global production, in the last years, of different metals or minerals reported in this paper, which include: iron [3], aluminum [4], boron [5], molybdenum [6], lithium [7], coal [8] and kaolin [9], among others.

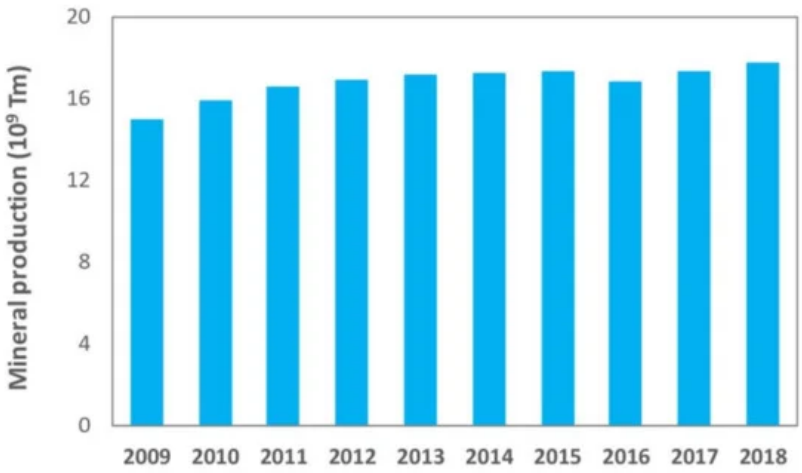

Figure 1. Evolution of world mineral production [2].

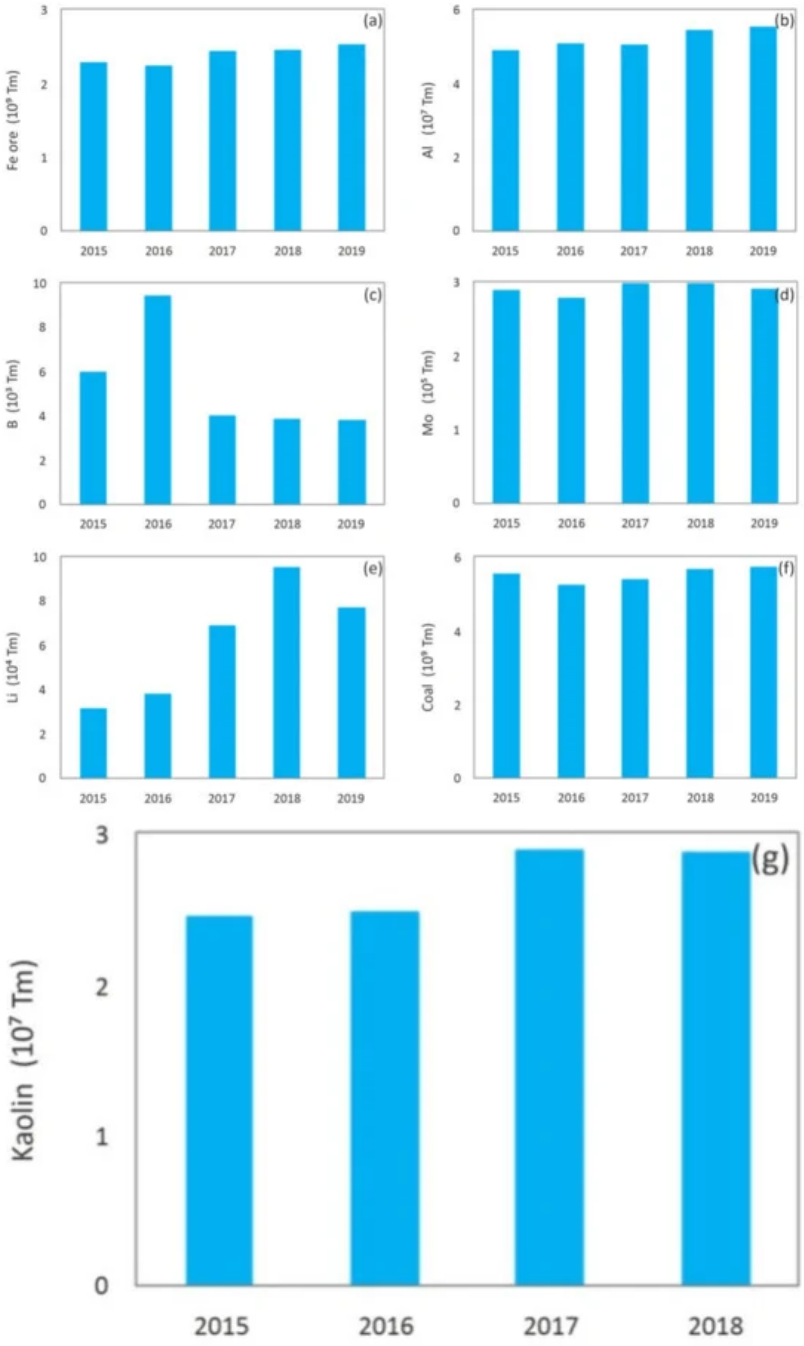

Figure 2. Worldwide production of: (**a**) Iron ore mineral [3]; (**b**) Countries with the largest smelter production of aluminum [4]; (**c**) Boron [5]; (**d**) Molybdenum [6]; (**e**) Lithium [7]; (**f**) Coal [8]; (**g**) Kaolin [9].

Thus, mining activities imply the generation of huge amounts of mining waste that produce great impacts on the environment, among others instability in waste dumps, acid drainage mainly due to oxidation processes, water pollution, air pollution and a long etcetera, which also includes the huge extents of territory occupied by the deposits of residues from the mineral washing and flotation plants [10][11].

Worldwide, there are approximately 3500 solid mining waste facilities, with an estimated generation of over 100 billion tons per year [12]. An idea of the magnitude of waste generated is given by the fact that, for example, in the case of iron or aluminum mining, the amount of solid waste generated is several times greater than the mass of the metals extracted, but in the case of noble metals such as gold, this ratio is greater than millions of times [13][14].

Tayebi-Khorami et al. [12] in an interesting study on the current management frameworks of mining waste, established the need for the mining industry to develop strategies in the medium and short term for proper management and use of waste aimed at achieving a lower environmental impact. The design and implementation of robust long-term solutions remains, to date, a challenge for the mining industry, due to the specificity of the sites where wastes are generated, the local weather conditions and the physicochemical heterogeneity of their wastes [15]. Besides, the global megatrends (large, social, economic, political, environmental, or technological changes) as driving technology demands should be taking into consideration by the mining industry for its future economic growth [16].

Solid mining waste is grouped into two main groups, viz mine waste rock (steriles) and tailings. Mine waste rock consists of low-grade excavated bedrock that has been transported to access profitable ore, and generally comprises of relatively coarse broken granular rock in the size range from sand to pebbles or boulders. They are mainly piled on high mounds which are porous, hydraulically unsaturated, and therefore highly exposed to atmospheric conditions (oxidation). Tailings are the main waste, both in volume and weight, generated in the process of concentrating minerals. Tailings are composed of process water and fines remaining after crushing and beneficiation of the ore, which may contain secondary materials from reactions with processing reagents, such as explosive agents or extraction chemicals [17]. Tailings streams are pumped into tailings storage facilities, TSFs (pools or dams) where they are deposited with low atmospheric exposure, which can even originate reducing conditions. Tailings can also be dried and stacked with the consequent displacement of the fines by the wind over long distances. The volume of tailings generated in the extraction of ore is almost equal to the volume of ore processed. It is estimated that there are approximately 1900 controlled TSFs worldwide in which 56×10^9 m^3 of mine tailings are stored. This volume is expected to increase up to 69×10^9 m^3 by 2025 [18]. The high volume of tailings stored at TSF gives rise to significant environmental problems resulting from the occupancy of large areas of land, including farmland and forests, and the consequent destruction of the landscape [19].

Moreover, tailings disposal also involves serious impacts on human health. In dry seasons, water from the surface of the tailings dams evaporates, leaving a fine, powdery material on the surface that pollutes the air in the surrounding areas. On the other hand, in rainy seasons, tailings deposits can collapse, causing landslides, with the consequent risk for the inhabitants of neighboring towns [20]. Over the past 40 years, numerous tailings dam collapses have occurred, resulting in significant impacts such as a prolonged suspension of mining activity, environmental degradation, damage to the image of the mining company, economic implications for the industry, legal implications and loss of human life [21]. Figure 3 shows shocking images of the collapse of several tailings dams.

Figure 3. Images of several environmental disasters produced by collapse of tailing dams: (**a**) collapse of tailings dam in Aználcollar, Spain, 1998 [22]; (**b**) Baia Mare disaster, Romania, 2000 [23]; (**c**) Mariana dam disaster, Brazil, 2015 [24]; (**d**) Brumadinho dam disaster, Brazil, 2019 [25].

Definitive solutions to the problem of mining waste are still far from being reached and much research and technological development must continue to be carried out. Although both types of waste present different geochemical behaviors, due to the large granulometric differences between them, different physical-chemical characteristics, and above all to the different storage practices, they can be considered, a priori, as a source of new exploitable materials [26].

In recent years, different studies have been carried out with the objective of recovering mining waste through their incorporation into different materials. Thus, nanostructured Mg(II)Al(III) layered double hydroxide (LDH) was manufactured from waste serpentine tailings by a chemical precipitation method [27]. Hexagonally ordered mesoporous silica materials were prepared from iron tailings by an innovative non-hydrothermal process at room temperature. These materials can be applied to energy storage or environmental protection [28]. Several studies have reported on the valorization of mining waste in building materials. In this way, iron ore waste was used as a complementary cementitious material to prepare colored composite cements more resistant to acid attack than Portland cement [29]; gold ore tailings were used as siliceous raw material for cement production [30]. For this application, the cementitious/pozzolanic properties of mineral tailings can be improved by activation methods [31]; molybdenum tailings have been investigated as replacement of fine aggregates in structural concrete [32]; and copper tailings were evaluated as raw material for geopolymer manufacture. Fluorite mines waste has been incorporated in the raw material mixture for the manufacture of glass [33], which allows for the incorporation of the potentially toxic elements of the tailings into the glass structure [34]. The valuation of mining waste

as fillers has also been considered in some studies. For instance, lead-zinc mill waste was studied as paste backfilling for an underground metalliferous mine [35]; and perlite wastes was used for the manufacture of lightweight materials by combining the geopolymerization technology with the foaming process [36]. A further recovery route investigated for these wastes is the production of synthetic stone. Thus, an artificial arenite was developed from different particle size fractions of the sandstone industry waste mixed with an unsaturated polyester resin [37]. Finally, as one of the potential recovery options, the manufacture of ceramic materials has been satisfactorily evaluated [38][39][40].The studies conducted to incorporate mine tailings into mullite-based ceramic materials are described hereafter.

Under the conventional model of the linear economy, taking into account the lowering of the ore grade and consequently higher excavation rates, the problem of mining waste and its associated inherent risks would continue to aggravate. In contrast, a circular economy articulates the importance of closed-loop systems that reduce the need for extraction and processing of new resources. As such, within mining activities and following the 3Rs principle of waste reduction (reduces, reuse, recycle), it can make an important contribution [41]. Thus, within the framework of the circular economy (which requires design for repair, reuse, recovery, refurbishment, restoration, and recycling) and the sustainable development objectives (ODS), many mining wastes could be considered, among others, as alternative materials in the construction sector instead of sources of pollution and risk. This solution will lead to the conservation of finite natural resources extensively used in the field of construction and to reduce the environmental impacts related to them [10][16][42][43]. Among construction materials, ceramic materials and, specifically those based on mullite, have been established as an appropriate alternative for the recovery of solid mining waste. The use of mining waste in the production of mullite-based ceramics contributes to various sustainable development objectives (ODS) of Agenda 2030, an action plan that resulted from the commitment of the member states of the United Nations, whose main objective is to ensure the protection of people, the planet and prosperity [44]. Thus, as far as objective 7 (affordable and clean energy) is concerned, the use of mining waste as a substitute for pure raw materials allows for a reduction in energy consumption. With regard to objective 13 (climate action), the recovery of waste contributes significantly to the reduction of CO_2 and other greenhouse gas emissions. Furthermore, the appropriate management and use of waste avoids negative impacts on terrestrial ecosystems, which are covered by objective 15 (life on land). But undoubtedly, the valorization of mining waste is closely linked to objective 12 (responsible consumption and production), which includes the achievement of a sustainable management and efficient use of natural resources by 2030, while considerably reducing waste generation through prevention, reduction, recycling and reuse activities.

According to the Mindat database [45], mullite (The name and chemical composition of the minerals and crystalline phases mentioned in this review are showed in Appendix A) is a nesosilicate, a group of silicates characterized by un-polymerized SiO_4 tetrahedrons, linked to one another by ionic bonds through interstitial cations. The chemical formula is $Al_{(4+2x)}Si_{(2-2x)}O_{(10-x)}$ where x = 0.17–0.59, and is composed of 38.00 wt.% aluminum, 13.18 wt.% silicon, and 48.82 wt.% oxygen, with the empiric formula $Al_{4.5}Si_{1.5}O_{9.75}$. Figure 4 shows the structure of mullite [46]. The mullite etymology is related to the place where it was found the first time in 1924, the Isle of Mull, Scotland, UK. Mullite is a crystalline phase of great technological importance due to its excellent technical properties, such as: low expansion and thermal conductivity (~4.5 × 10^{-6} °C^{-1} and 6 kcal·m^{-1}·h^{-1} °C^{-1} at 20 °C, respectively), and appropriate fracture strength and toughness (~200 MPa y ~2.5 MPa $m^{1/2}$, respectively) [47]. In addition, it features high creep resistance, corrosion stability and thermal stability. All these features currently make mullite to be, probably, one of the most important phases in traditional and advanced ceramic. Monolithic mullite ceramics find application in tableware [48], porcelain stoneware [49][50], refractory [51] or electronic devices [52]. Mullite coatings have been used successfully as environmental barrier coatings for the protection against oxidizing agents, reducing agents or aggressive chemicals at high temperatures [53][54]. Besides ceramic or metallic surfaces, mullite composites, including composites prepared with mullite matrix or mullite fiber, find important applications as components in turbine engines, high-performance furnaces or heat shields for space vehicles [55][56][57].

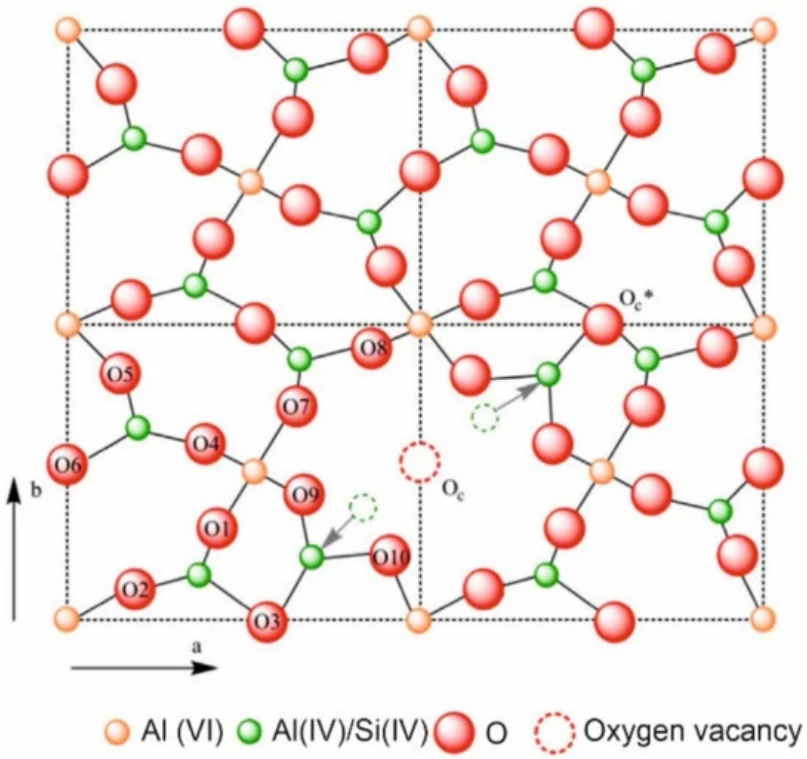

Figure 4. Crystal structure of mullite along c-axis [46].

Mullite is a mineral not very abundant in nature since high temperature and low pressure conditions are required for its formation. Due to its high technological demand, mullite has to be manufactured by synthetic methods, rather than being mined. For the synthesis of mullite, there are three basic routes, namely: sintering, melting and chemical processing [58].

- Sinter-mullite. Through sintering processing, mullite is basically obtained by reactions in the solid state by interdiffusion of aluminum, silicon and oxygen atoms. The aluminum-bearing raw materials used for the synthesis of mullite are mainly clay minerals, basically kaolinite ($Al_2Si_2O_5(OH)_4$) and pirofilite ($4SiO_2{\cdot}Al_2O_3{\cdot}H_2O$); other minerals such as Al_2SiO_5 (sillimanite, cianite and andalusite); AlO(OH) (boehmite and diaspore); gibbsite ($Al(OH)_3$) and bauxite ($(AlO_x(OH)_{3-2x}$) with x = 0–1) are usually added as supplementary raw materials. Quartz (SiO_2) is used as Si source. During sintering at ~500 °C, kaolinite is transformed into metakaolinite ($Al_2Si_2O_7$) by the loss of structural molecules of water. Later, at higher temperature (~980 °C) metakaolinite is decomposed in Si-Al spinel and amorphous silica. The reaction between these two phases at~1200 °C origins the formation of mullite [50]. For the complete transformation of kaolinite into mullite by the sintering process, very high temperatures are required (1600–1700 °C) due to the diffusion coefficient of mullite in the grain border being very low. To reduce the mullitization temperature, it is convenient to use systems to mix raw materials at the atomic level.

- Fused-mullite. Mullite is synthesized by fusing of raw materials (alumina Bayer, quartz sand, rock crystal and fused silica) in an electric furnace at a temperature over 2000 °C until homogeneous molten is achieved. By controlled crystallization during the cooling, molten mullite is developed [59].

- Chemical-mullite. This method comprises the use of different chemical processes such as sol-gel technologies [60], precipitation [61], hydrolysis [62], pyrolysis [63] or cool vapor deposition techniques (CVD) [64].

Accordingly, the synthesis of mullite is an expensive process due to the requirement of high temperature or complex synthesis methods. On the other hand, the kaolin world reserves are drastically decreasing, because their demand for the production of paper and ceramic building materials (principally ceramic tiles). For both reasons, during the two last decades, research efforts have been conducted to study the synthesis of mullite from less common and low cost raw materials such as inorganic waste from different sources and characteristics. Thus, waste from the agro-food industry (rice husk ash) [65][66], spent cracking catalysts [67][68][69], aluminum buffing dust [70], aluminum sludge generated in water treatment plants [71], ceramic wastes from the manufacture of ceramic tiles [72] or fly ash [73][74], among others have been investigated as raw materials for the synthesis of mullite.

Furthermore, the valorization of mining waste by the production of mullite-based ceramic materials has also been the object of scientific interest. The aim of this work is to carry out a review of the scientific production performed in recent years on the use of waste rock and tailings from the mining industry in the manufacture of ceramic materials in which mullite is developed as one of the main crystalline phases. In this sense, the review includes mining waste from the extraction of metals (iron, aluminum, boron, molybdenum and lithium) and minerals (coal gangue, kaolin and ornamental rocks).

2. Mining Waste from the Extraction of Metals

2.1. Iron Mining Waste

Iron is the most frequently used metal in the world. As the main component of steel, it is an essential element in different sectors such as the automobile, construction industry, engineering or equipment production. In 2019, world iron production was approximately 2.5 × 10^9 metric tons, with Australia and Brazil, with 930 × 10^6 and 480 × 10^6 metric tons respectively, being the largest producers [3]. Possible ways of recovering the iron mining waste include its use as catalysts for the synthesis of carbon nanomaterials [75], ceramic additive [76] and its incorporation into cement [29], concrete [77] or geopolymers [78]. The main results of the aimed at the synthesis of mullite-based ceramics from iron mining waste are described hereafter. Table 1, Table 2 and Table 3 list the chemical composition of the iron waste, the processing parameters and the technological properties of the developed ceramic materials.

Table 1. Chemical composition (expressed wt.% oxide) of iron mining waste.

Reference	SiO_2	Al_2O_3	Fe_2O_3	CaO	MgO	Na_2O	K_2O	TiO_2	P_2O_5	MnO	LOI
[79]	39.40–63.32	1.22–1.42	32.31–55.61	0.08–0.36	---	---	---	---	---	---	2.33–3.42
[80]	19.84–21.63	11.91–13.25	66.15–72.21	---	0.71–0.84	---	1.25–1.53	---	---	---	nd
[81]	24.4	10.95	44.52	6.2	0.99	0.28	0.86	0.42	2.78	---	6.95
[82]	15.78–20.45	13.19–18.81	57.32–67.44	0.18–0.34	---	---	0.21–0.28	---	0–0.66	1.49–2.62	7.3–9.4

Table 2. Experimental conditions used in the development of mullite-based materials from iron mining waste.

Reference	Percentage of Use (wt.%)	Additional Raw Materials (wt.%)	Shaping Method	Sintering Conditions
[79]	30–50	Clay (35–60) Fluxing minerals (0–15)	UP; 25–30 MPa ∅ 50 mm 110 × 55 mm	1060–1200 °C 10 °C/min
[80]	60	Kaolinitic clay (40)	UP; 30 MPa 50 × 50 mm 110 × 55 mm	850–1000 °C 1 h
[81]	50–70	Kaolin (25) Quartz sand (5–25)	UP; 20 MPa 60 × 35 × 5 mm	1150–1250 °C 5 °C/min; 30 min
[82]	100	nr	UP; 10 MPa 50 × 50 × 5 mm	1200 °C 10 °C/min; 2 h

Table 3. Technological properties of mullite-based materials developed from iron mining waste.

Reference	Final Material	Compressive Strength (MPa)	Flexural Strength (MPa)	Water Absorption (%)	Apparent Density (g/cm^3)	Firing Shrinkage (%)
[79]	Ceramic tiles	nd	17–31	<0.5–16.5	nd	0.07–7.00
[80]	Ceramic bricks and pavement blocks	15–70	nd	6–8	2.4–2.7	nd
[81]	Porcelain tiles	nd	30–75	<0.5–17	nd	5–16
[82]	Porcelain tiles	nd	53.41	0.34	3.63	26.51

Das et al. [79] investigated the potential of iron ore tailings as a raw material in the manufacture of ceramic tiles for pavement and flooring. The iron ore tailings were mainly composed of SiO_2 and Fe_2O_3 along with Al_2O_3 as a minority component. From a mineralogical point of view, the main components of iron tailings were hematite (Fe_2O_3), quartz and kaolinite, while illite ($(K,H_3O)(Al, Mg, Fe)_2(Si,Al)_4O_{10}$), goethite (FeO(OH)) and montmorillonite ($(Na,Ca)_{0.3}(Al,Mg)_2Si_4O_{10}(OH)_2 \cdot nH_2O$) were identified as minor crystalline phases. The composition containing 40 wt.% tailings, 50 wt.% clay and 10 wt.% flux presented, after firing, a water absorption value lower than 0.5%. The mineralogical composition of the fired tiles was mostly composed of quartz and mullite, with fayalite and anorthite as the minor phases. In terms of its microstructure, it was formed by crystalline phases embedded in a glassy matrix with a homogeneous distribution of pores. All these characteristics enabled these ceramic tiles to be used as glazed tiles suitable for both domestic and industrial floors. In a later study, Gosh et al. [80] informed about the manufacture of ceramic bricks and paving blocks from iron ore tailings. The chemical composition consisted of SiO_2, Fe_2O_3 and Al_2O_3 as the major oxides and MgO and K_2O as the minor components. As concerns the mineralogical composition, the iron ore tailings consisted of magnetite ($Fe^{2+}Fe^{3+}{}_2O_4$, 2.4–6.9 wt.%), hematite (0–48.6 wt.%), goethite (30.1–77.6 wt.%), kaolinite (13.7–17.3 wt.%) and quartz (0.7–2.7 wt.%). The paste composition made up of 60 wt.% iron tailings and 40 wt.% kaolinitic clay gave rise after firing to dense materials composed of hematite (72.3–74.1 wt.%,), mullite (2.3–8.4 wt.%) and quartz (19.3–23.6 wt.%). The authors pointed out the possibility of manufacturing ceramic bricks and blocks with adequate technological properties at lower temperatures than commercial materials composed of 100 wt.% of clay, which results in savings in production costs. Chen et al. [81] studied the possibility of manufacturing red porcelain tiles with hematite tailings as a substitute for feldspar ($(K,Na,Ca,Ba,NH_4)(Si,Al)_4O_8$). The major constituents of the tailings were Fe_2O_3, SiO_2, Al_2O_3 and CaO, with quartz and hematite being the main crystalline phases; calcite ($CaCO_3$) and chlorite ($Na_{0.5}Al_4Mg_2Si_7AlO_{18}(OH)_{12} \cdot 5H_2O$) were also identified as minority phases. The study indicated that the incorporation of tailings promoted the formation of liquid phases and led to a decrease in the sintering temperature of the samples, although it was necessary to optimize their content in the ceramic pastes since an excessive percentage of tailings reduced the densification temperature range. Materials fired at 1200°C from the composition consisting of 55–65 wt.% tailings, 25 wt.% kaolin and 10–20 wt.% quartz sand proved to be the most appropriate for obtaining porcelain tiles with suitable technological properties. The fired tiles were made up of quartz, hematite, cristobalite (SiO_2), mullite and anorthite ($CaAl_2Si_2O_8$) and had a dense microstructure with low porosity.

Recently, Fontes et al. [82] reported the use of iron tailings in the manufacture of porcelain tiles. The tailings were separated into three fractions by a dry segregation procedure. In this way, the fractions, namely, iron ore, quartz sand and a fraction collecting the concentrates of the clay minerals, were obtained. The latter presented a series of physical-chemical characteristics that made it more suitable than the original iron tailings for the manufacture of porcelain tiles, without the addition of auxiliary raw materials. Thus, its chemical composition, consisting mainly of Fe_2O_3, SiO_2 and Al_2O_3 was located in the region of mullite formation in the SiO_2-Al_2O_3-FeO/Fe_2O_3 ternary diagram. The incorporation of iron tailings led to the formation of a higher amount of liquid phases during firing. Moreover, it had a smaller particle size, which facilitated the shaping of the pieces (plasticity). The fired tiles were made up of hematite (72.2 wt.%) together with mullite (17.7 wt.%), cristobalite (7.1 wt.%) and an amorphous phase (3.2 wt.%) and showed a porosity of approximately 5%, with 1.3% corresponding to open porosity. This low value of porosity was reflected in a water absorption (0.34%) that met the requirements for tiles in the group (BIa) (dry pressed tiles with very low water absorption (<0.5%). These tiles also showed good mechanical behavior.

2.2. Aluminum Mining Waste

Nowadays, over 90% of the world's aluminum production is achieved by the hydrometallurgical extraction and refining of the alumina contained in bauxite, through the Bayer process [83]. In this process, the bauxite ore, previously ground, is digested at high temperature in a highly caustic solution. At the completion of the digestion, there is a suspension containing an aluminate solution together with sand (material size >100 µm) and red sludge (fine particles). From this suspension, an aluminum hydrate is separated by precipitation, which is then washed, dried and calcined to yield alumina as the final product of the process. In the Bayer process, a sludge consisting of a mixture of metal oxides is produced as a by-product. This sludge is red in color due to its high iron oxide content. It is estimated that in the production of 1 ton of alumina, 2 tons of red sludge are originated [84]. In 2019, world alumina production was 133×10^6 metric tons, headed by China (73×10^6 metric tons) followed by Australia (20×10^6 metric tons) [85]. Therefore, the amount of red sludge generated in 2019 as a by-product of the Bayer process is estimated to be around 250×10^6 metric tons. In view of the huge production of this waste, numerous studies have investigated its recovery of different applications [86], such as: asphalt binders [87], cement industry [88], geopolymers manufacture [89], ceramic bricks and tiles [90][91] and aluminosilicate glass [92]. Amongst these investigations, those aimed to valorize waste generated in the Bayer process in the production of mullite-based ceramic materials are described hereafter. Table 4, Table 5 and Table 6 show the chemical composition of Bayer waste, the processing parameters and the technological properties of the developed ceramic materials.

Table 4. Chemical composition (expressed wt.% oxide) of waste generated in the Bayer process.

Reference	Waste	SiO_2	Al_2O_3	Fe_2O_3	CaO	Na_2O	K_2O	TiO_2	SO_3	LOI
[93][94]	Red mud	33.57	27.66	7.56	15.26	3.54	1.76	3.36	---	7.29
[95]	Alumina waste	1.40	90.90	---	---	---	---	---	7.00	nd

Table 5. Experimental conditions used in the development of mullite-based materials from waste generated in the Bayer process.

Reference	Mining Waste	Percentage of Use (wt.%)	Additional Raw Materials (wt.%)	Shaping Method	Sintering Conditions
[93]	Red mud	65.8–7.0	Kaolin (28.2–30) Ammonium molybdate (0–6)	UP; 25 MPa ∅ 25 mm 70 × 6 × 6 mm	1150–1200 °C 3 °C/min; 2 h
[94]	Red mud	23–29	SiC (35–44) $Al(OH)_3$ (15) V_2O_5 (3) AlF_3 (4) Graphite (5–20)	UP; 20 MPa 35 × 10 mm	1150–1350 °C 2 °C/min; 3 h
[95]	Alumina waste	48–56	Kaolin (44–52)	UP; 33–66 MPa 30 × 5 × 5 mm	1450–1500 °C 5 °C/min; 1 h

Table 6. Technological properties of mullite-based materials developed from waste generated in the Bayer process.

Reference	Mining Waste	Final Material	Flexural Strength (MPa)	Water Absorption (%)	Apparent Density (g/cm^3)	Firing Shrinkage (%)
[93]	Red mud	Ceramic floor tile	153–195	7–27	1.45–1.83	nd
[94]	Red mud	SiC/mullite composite porous ceramics	8–68	nd	nd	nd
[95]	Alumina waste	Porous mullite blocks	46–56	17–18	nd	10–11

Wang et al. [93] studied the manufacture of low-cost pavement tiles from red sludge with additions of kaolin and ammonium molybdate ($(NH_4)_6Mo_7O_{24}$). The results revealed that ammonium molybdate acted as a catalyst for the formation of mullite crystals, promoting sintering at lower temperatures while increasing the rate and degree of reaction. The microstructure of the samples sintered at 1180 °C was comprised of anisotropic mullite crystals, approximately 10 mm in length, together with some anorthite crystals. These materials showed a high flexural strength (195 MPa) attributed to the higher fracture energy absorption by the mullite interlocked crystals. Those ones sintered at temperatures higher than 1180 °C presented a significant decrease in technological properties as a result of the increase in the amount of the glassy phase and the existence of intercrystalline pores. The authors pointed out that the use of ammonium molybdate as a catalyst promoted the formation of fine Al_2O_3 crystals with high chemical reactivity. In turn, it generated MoO_3, which reduced the viscosity of the silica-rich liquid phase. Therefore, the dissolution of Al_2O_3 in the liquid phase was favored and consequently, the nucleation of mullite crystals. In a later study, the authors investigated the use of this same residue as a starting material for the synthesis of SiC/mullite composite porous ceramics [94]. For this, they used aluminum hydroxide ($Al(OH)_3$), Bayer red sludge and silicon carbide (SiC) as raw materials and studied the effect of V_2O_5 and AlF_3 as catalysts for the development of low temperature mullite. The composite materials included 6H-SiC, mullite, cristobalite and alumina as crystalline phases. The authors pointed out a significant increase in the amount of mullite from 1250 °C, at the expense of the decrease of alumina in the sintered samples, which caused an improvement in the bending strength, as well as the reduction in the porosity. The microstructure consisted of rod-shaped mullite crystals and plate-shaped SiC grains distributed among the mullite particles. The samples sintered at 1350 °C showed optimum behavior, with a bending strength of 49.4 MPa and a porosity of 31.4%. The authors highlighted that the introduction of V_2O_5 and AlF_3 changed the mechanism of the mullite formation reaction, significantly reducing the sintering temperature. Thus, AlF_3 is converted into vapor phase fluorine and reacts with aluminum oxide and silicon oxide to generate SiF_4 and AlOF, respectively. In this way, the growth of the crystal nucleus is accelerated along an axis, causing the quick formation of a significant amount of mullite crystals.

In addition to the red sludge, the Bayer process generates an alumina-rich residue (90 wt.%), which can be used as a source of alumina in the manufacture of porcelain. Da Silva et al. [95] reported the manufacture of porous mullite blocks from mixtures of kaolin and Bayer alumina waste. The alumina waste consisted mainly of Al_2O_3, with SiO_2 and SO_3 as minor components. Regarding its mineralogical composition, in addition to alumina, the waste contained Na_2O and sulfur phases as impurities. Mixtures of kaolin and alumina residue were formulated to achieve the stoichiometry of mullite 3:2. After firing, all samples included mullite as the main crystalline phase, together with corundum (α-alumina) and quartz. The mullite content was increased by the firing temperature, resulting in an enhancement of the mechanical properties of the fired materials. The microstructural study revealed the bimodal growth of primary mullite acicular crystals, developed in the glass matrix, and smaller crystals of secondary mullite (Figure 5). The authors highlighted the possibility of recovering Bayer's alumina residue to produce mullite materials suitable for applications requiring high porosity and strength at high temperatures.

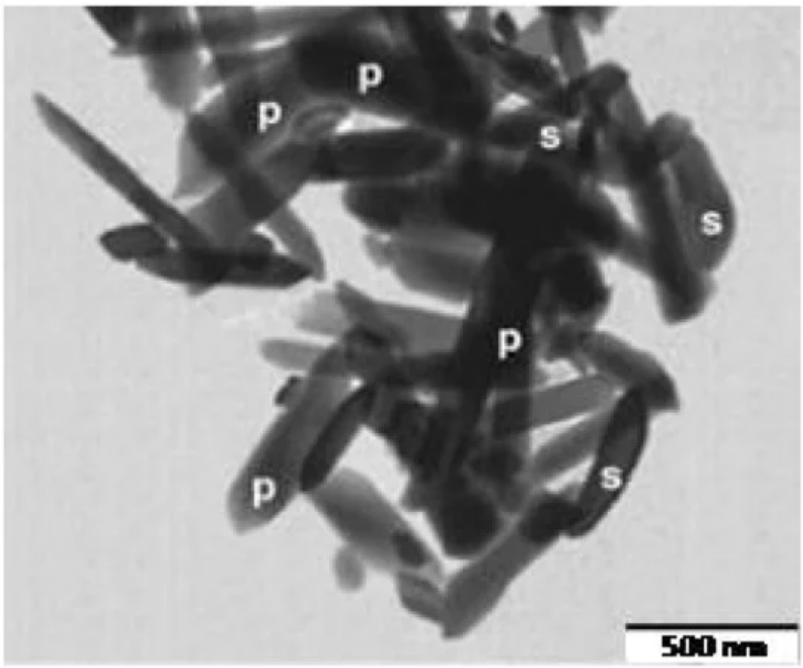

Figure 5. TEM image of the mullite crystals developed at 1450 °C in porous mullite blocks from Bayer alumina waste and kaolin (p and s denotes primary and secondary mullite, respectively) [95].

2.3. Boron Mining Waste

Boron is mainly demanded for the manufacture of fiberglass. However, it is also an essential element in agriculture (herbicides and pesticides) and in the production of ceramic materials, borosilicate glass and detergents [96]. Other uses of boron include the manufacture of special steels with high resistance to impact, and also its application in the field of atomic energy. Because of its high neutron absorption capacity, it is used as a control buffer in nuclear reactors and as a constituent material of neutron shields. In 2019, world production of boron was approximately 3.8×10^6 metric tons, being led by Turkey with 2.5×10^6 metric tons [5]. Studies on the valorization of boron mining wastes have focused mainly on the development of cement [97], concrete [98] and geopolymers [99]. However, some research has explored its incorporation into mullite-based ceramic materials, as detailed below. Table 7, Table 8 and Table 9 present the chemical composition of boron mining wastes, processing parameters and technological properties of the ceramic materials developed.

Table 7. Chemical composition (expressed wt.% oxide) of boron mining wastes.

Reference	Waste	SiO_2	Al_2O_3	Fe_2O_3	CaO	MgO	Na_2O	K_2O	B_2O_3	LOI
[100]	(1)	15.83	1.06	0.24	20.66	19.84	2.58	0.63	3.99	34.75
[101][102]	(2)	0.39–19.81	0.11–0.74	0.13–0.33	23.31–52.75	0.60–8.96	0.00–1.34	0.00–0.17	16.37–31.11	14.68–30.74

Table 8. Experimental conditions used in the development of mullite-based materials from boron mining wastes.

Reference	Mining Waste	Percentage of Use (wt.%)	Additional Raw Materials (wt.%)	Shaping Method	Sintering Conditions
[100]	Tincalconite	2–16	Clay (60) Feldespatic waste (24–40)	UP; 16 MPa 110 × 55 × 6 mm	1050–1150 °C 2 °C/min; 1 h
[101]	Colemanite	1–14.80	nr	UP 15 × 5 × 5 mm	1120–1195 °C 4 min
[102]	Colemanite	1.10–8.56	nr	UP ∅ 50 mm 5 × 10 cm	1180–1230 °C 4 min

Table 9. Technological properties of mullite-based materials developed from boron mining wastes.

Reference	Mining Waste	Final Material	Flexural Strength (MPa)	Water Absorption (%)	Firing Shrinkage (%)
[100]	Tincalconite	Terracota tiles	16–44	0.1–14	3.0–8.5
[101]	Colemanite	Wall and floor tiles	38.43	0.49	6.8
[102]	Colemanite	Porcelain tiles	44.80	0.01	7.4

Kurama et al. [100] investigated the production of terracotta tiles with improved physical-mechanical properties and lower production costs, using the tincalconite sieve dewatering residue (TSW) generated in the manufacture of borax ($Na_2B_4O_5(OH)_4]\cdot 8H_2O$) from the mineral tincalconite ($Na_2B_4O_4(OH)_4\cdot 3H_2O$). It is estimated that 0.5 t of this waste is produced in the production of 1 t of borax. TSW was composed of SiO_2, CaO and MgO as major oxides and Al_2O_3, B_2O_3 and alkaline oxides as minor components. In terms of mineralogy, TSW was comprised of dolomite ($CaMg(CO_3)_2$, tincalconite, montmorillonite and calcite. The authors noted that the water absorption of fired materials decreased considerably when the TSW content in the paste composition increased, which was attributed both to the strong melting action of its B_2O_3 content and to the sintering-promoting character of the alkaline earth oxides (MgO and CaO), whose content in this waste was considerably higher than in the other constituent raw materials. As a consequence, the bending strength was also increased by the TSW content in the composition. The main crystalline phase in the fired materials was quartz, which was largely a remnant of the initial quartz contained in the raw materials. As for the newly formed phases, mullite was the main crystalline phase developed during firing. The study also showed that the content of the amorphous phase increased regularly as the amount of TSW incorporated into the composition increased. However, Cicek et al. [101] considered that the use of tincalconite extraction/enrichment tailings into the ceramic tile manufacturing sector was not feasible, as they contain a high percentage of Na_2O, which is a very energetic flux and provides excessive fluidity to the ceramic body. Therefore, its use in industrial ceramic tile production, where a fast-firing cycle with very fast heating and cooling speeds is applied, is not feasible. Therefore, they developed pavement and covering ceramic tiles using tailings from the manufacture of boric acid (H_3BO_3) from the mineral colemanite ($CaB_3O_4(OH)_3\cdot H_2O$). In this case, new formulations of floor ceramic tiles were prepared with percentages of alkaline earth oxides and SiO_2/Al_2O_3, Na_2O/K_2O and MgO/CaO ratios similar to those of commercial compositions. The authors noted that compositions containing 5.66 wt.% colemanite tailings presented a densification temperature 65 °C below that used in the manufacture of ceramic floor tiles. The B_2O_3 content in the tailings favored the generation of liquid phases, thus facilitating viscous sintering at a slightly lower temperature than that used in commercial manufacture. The major crystalline phases were anorthite, albite ($Na(AlSi_3O_8)$), mullite and quartz. Plagioclase formation ($(Na,Ca)(Si,Al)_3O_8$) was promoted by the high Ca content of the boron tailings. These tiles showed shrinkage during firing similar to standard tiles and presented lower water absorption values (0.49%). However, the bending strength (38.43 MPa) decreased considerably with respect to commercial floor tiles due to the formation of excess plagioclase, which is harder but less resistant. In a recent study, Karadagli and Cicek [102] studied the introduction of this same colemanite tailing in the manufacture of porcelain stoneware tiles. They incorporated 3–10 wt.% of tailings into a formulation used for commercial production of porcelain tiles. The authors achieved a decrease in the sintering temperature of 38 °C. The new tiles showed bending strength (44.80 MPa) and water absorption (0.01%) values complying with the requirements for porcelain tile.

2.4. Molybdenum Mining Waste

Molybdenum is mainly used for the manufacture of resistant steels, but it is also required as a component of superalloys, nickel alloys and in other industrial sectors such as lubricants, chemicals and electronics. World production of molybdenum in 2019 was 290×10^3 metric tons [6], with production being led by China with 130×10^3 metric tons [103]. In the literature, the works focused on the valorization of Mo mining wastes are scarce, being focused on its incorporation in cement and concrete [104][105]. Moreover, Karhu et al. [106] investigated the use of molybdenum tailings as raw materials for

producing mullite-based ceramics. Table 10 displays the chemical composition, processing parameters and technological properties of the ceramic materials. Molybdenum tailings were mainly composed of SiO_2 and Al_2O_3 and a considerable content (22 wt.%) of minor components (CaO, Fe_2O_3, K_2O, Na_2O and MgO). The main mineral phases were quartz (40 wt.%), albite (23 wt.%) and andesite ($(Ca,Na)Al_2Si_2O_8$, 12 wt.%), together with minor amounts of K-feldspar (6 wt.%), biotite ($K(Mg,Fe^{2+})_6(Si,Al)_8O_{20}(OH)_4{\cdot}nH_2O$, 6 wt.%) and muscovite ($KAl_2(Si_3Al)O_{10}(OH)_2$, 3 wt.%). Sintering of tailings and boehmite mixtures resulted in crystalline materials including mullite as the main crystalline phase, along with corundum and amorphous phase. The microstructure of these materials was composed of acicular mullite crystals surrounded by a glassy phase. During sintering, the alkali and K-mica feldspars contained in Mo tailings led to a liquid phase that facilitated the reaction of the silica with the alumina caused by the thermal decomposition of boehmite and the subsequent crystallization of mullite.

Table 10. Chemical composition (expressed wt.% oxide), processing parameters and technological properties of ceramic materials developed from molybdenum mining waste.

eference	SiO_2	Al_2O_3	Fe_2O_3	CaO	MgO	Na_2O	K_2O	LOI
	73.2	11.1	2.93	1.95	4.84	3.45	1.51	nd
[106]	Final material	Percentage of use (wt.%)	Additional raw materials (wt.%)	Shaping method	Sintering conditions	Compressive strength (MPa)	Apparent density (g/cm^3)	
	Mullite-based ceramics	33.6–83.5	Boehmite (16.5–66.4)	UP; 25 MPa 20 × 3 mm	1300 °C 3.3 °C/min; 3h	~62	2.7	

2.5. Lithium Mining Waste

In the last years, lithium has become one of the key chemical elements for new technologies. Although lithium has long been used in different industrial sectors, the development of lithium-ion batteries has resulted in lithium becoming a key mineral, as lithium batteries are essential for the development of smartphones, laptops, hybrid and electric cars or rechargeable devices, such as solar charging lithium ion batteries. World lithium production in 2019 was 77,000 metric tons, with Australia (42,000 metric tons) and Chile (18,000 metric tons) being the major producers [107]. By 2025, the global demand for lithium is estimated to be 820,000 metric tons of lithium carbonate equivalent [108]. One of the main routes of lithium extraction is acid roasting with H_2SO_4 of the mineral spodumene ($LiAlSi_2O_6$), which contains approximately 8% of Li_2O [109][110][111]. Lemougna et al. [112] studied the use of quartz feldspar sand (QFS) residues originating during the chemical production of lithium from spodumene as a raw material for the manufacture of porcelain and structural materials. Table 11 shows the chemical composition of this waste together with the processing parameters and technological properties of the final ceramic materials.

Table 11. Chemical composition (expressed wt.% oxide), processing parameters and technological properties of ceramic materials developed from lithium mining waste.

Reference	SiO_2	Al_2O_3	Fe_2O_3	CaO	P_2O_5	Na_2O	K_2O	LOI
	77.50	13.5	0.20	0.30	0.10	4.80	3.30	0.0
	Final material	Percentage of use (wt.%)	Additional raw materials (wt.%)	Shaping method	Sintering conditions			
	Porcelain materials	41–50	Kaolin (50) Quartz (0–9)	Slip casting 80 × 20 × 20 mm	1050–1200 °C 5 °C/min; 2 h			
[112]	Structural materials	80–90	Kaolin (10–20)	Slip casting 80 × 20 × 20 mm	1050 °C 5 °C/min; 2 h			
	Final material	Compressive strength (MPa)	Flexural strength (MPa)	Water absorption (%)	Apparent density (g/cm^3)	Firing shrinkage (%)		
	Porcelain materials	40–90	10–30	0.2–18	1.7–2.5	2–18		
	Structural materials	67–69	16.5–17.5	6.3–6.8	2.05–2.07	nd		

The QFS residue was composed of SiO_2 as the major oxide and Al_2O_3, and alkaline oxides as minor components. From a mineralogical point of view, spodumene waste included albite (44 wt.%), quartz (32 wt.%), microcline ($KAlSi_3O_8$; 11 wt.%) and muscovite (6 wt.%) together with amorphous phase (7 wt.%) (Figure 6). The porcelain materials obtained after a sintering process were mainly composed of quartz (13–26 wt.%), mullite (12–20 wt.%) and amorphous phase (42–56 wt.%), the highest percentages of mullite being obtained for materials sintered at 1200 °C (Figure 7). These materials presented the best technological properties, with a dense and compact microstructure with microstructural characteristics similar to those of reference porcelain compositions. The highest compressive strength values of 90 MPa fulfilled the requirements for fired bricks, masonry bricks and ceramic pavers exposed to light traffic. As regards to bending strength, maximum values of 30 MPa were achieved, which are slightly lower than those presented by commercial porcelain stoneware tiles. Materials sintered at 1200 °C showed very low water absorption values (0.2%) corresponding to an apparent density of 2.5 $g \cdot cm^{-3}$, both properties being comparable to those reported in studies of porcelain materials. The shrinkage values on sintering were also similar to the values of approximately 20% shrinkage reported for some porcelain compositions fired at 1200 °C. As for the properties of structural materials manufactured with 80 and 90 wt.% of spodumene tailings, they exhibited values of compressive strength exceeding 17–20 MPa, which is the value required for ceramic pavers subjected to light traffic. Similarly, they showed water absorption well below 15%, complying with the requirement for ceramics with construction applications.

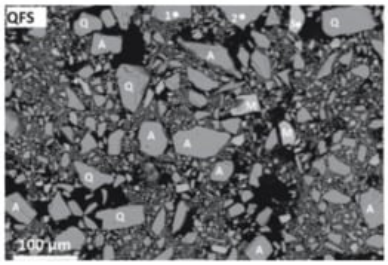

Element (wt.%)	1: Quartz (Q)	2: Albite (A)	3: Microcline (M)
O	48.44	44.12	41.65
Si	51.56	35.42	32.97
Al	-	11.52	10.68
Na	-	8.95	0.43
K	-	-	14.27

Figure 6. SEM of QFS powder [112].

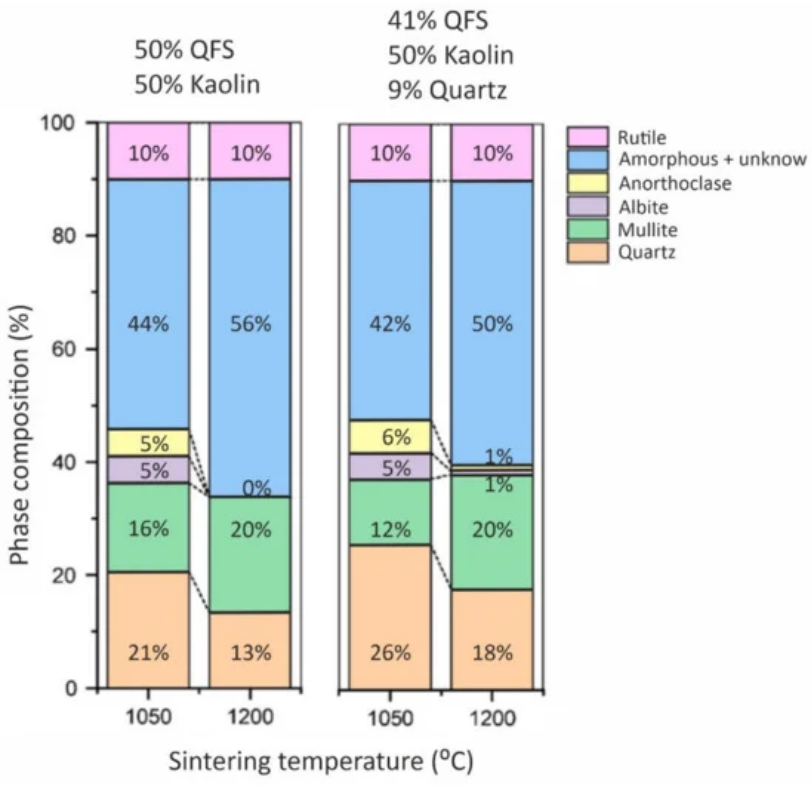

Figure 7. Phase composition of investigated compositions at indicated temperatures [112].

References

1. Elshkaki, A.; Graedel, T.E.; Ciacci, L.; Reck, B. Copper demand, supply, and associated energy use to 2050. Glob. Environ. Chang. 2016, 39, 305–315.
2. Evolución Anual de la Producción Mundial de Minerales de 2005 a 2018. Available online: (accessed on 2 February 2021).
3. Major Countries in Iron Ore Mine Production by Country 2015–2019. Available online: (accessed on 2 February 2021).

4. Countries with the Largest Smelter Production of Aluminum from 2015 to 2019. Available online: (accessed on 8 February 2021).
5. Major Countries in Boron Production from 2015 to 2019. Available online: (accessed on 2 February 2021).
6. Mine Production of Molybdenum Worlwide from 2010 to 2019. Available online: (accessed on 2 February 2021).
7. Lithium Mine Production Worldwide from 2010 to 2018 (in Metric Tons of Lithium Content). Available online: (accessed on 2 February 2021).
8. Coal Production Worldwide from 1998 to 2019 (in Exajoules). Available online: (accessed on 8 February 2021).
9. Brown, T.J.; Idoine, N.E.; Wrighton, C.E.; Raycraft, E.R.; Hobbs, S.F.; Shaw, R.A.; Everett, P.; Kresse, C.; Deady, E.A.; Bide, T. World Mineral Production 2014–2018, 2020th ed.; British Geological Survey: Keyworth, Nottingham, UK, 2020; ISBN 978-0-85272-788-1.
10. Amrani, M.; Taha, Y.; El Haloui, Y.; Benzaazoua, M.; Hakkou, R. Sustainable reuse of coal mine waste: Experimental and economic assessments for embankments and pavement layer applications in Morocco. Minerals 2020, 10, 851.
11. Terrones-Saeta, J.M.; Suárez-Macías, J.; Linares Del Río, F.J.; Corpas-Iglesias, F.A. Study of copper leaching from mining waste in acidic media, at ambient temperature and atmospheric pressure. Minerals 2020, 10, 873.
12. Tayebi-Khorami, M.; Edraki, M.; Corder, G.; Golev, A. Re-thinking mining waste through an integrative. Minerals 2019, 9, 286.
13. Rankin, W.J. 16 Towards zero waste. In Minerals, Metals and Sustainability: Meeting Future Material Needs; CSIRO Publishing: Victoria, Australia, 2011; pp. 459–525. ISBN 9780643097261.
14. Rankin, W.J. Towards Zero Waste. AusIMM Bull. 2015, 2015, 32–37.
15. Vriens, B.; Plante, B.; Seigneur, N.; Jamieson, H. Mine waste rock: Insights for sustainable hydrogeochemical management. Minerals 2020, 10, 728.
16. Glavic, P.; Pintaric, Z.N.; Bogataj, M. Process desing and sustainable development—A european perspective. Processes 2021, 9, 148.
17. Adiansyah, J.S.; Rosano, M.; Vink, S.; Keir, G. A framework for a sustainable approach to mine tailings management: Disposal strategies. J. Clean. Prod. 2015, 108, 1050–1062.
18. Global Tailings Portal. Available online: (accessed on 2 February 2001).
19. Sun, W.; Ji, B.; Khoso, S.A.; Tang, H.; Liu, R.; Wang, L.; Hu, Y. An extensive review on restoration technologies for mining tailings. Environ. Sci. Pollut. Res. 2018, 25, 33911–33925.
20. Xu, D.M.; Zhan, C.L.; Liu, H.X.; Lin, H.Z. A critical review on environmental implications, recycling strategies, and ecological remediation for mine tailings. Environ. Sci. Pollut. Res. 2019, 26, 35657–35669.
21. Davies, M.P. Impounded mine tailings: What are the failures telling us? Can. Min. Metall. Bull. 2001, 94, 53–59.
22. Martí, J. 20 Years Since Aznalcóllar: Lessons Learned. Available online: (accessed on 22 March 2021).
23. SBS World News Australia Is Cyanide Safe to Use in Mining? Available online: (accessed on 22 March 2021).
24. Alvés, R. Dozens Missing in Brazil Mine Disaster, Death Toll Uncertain. Available online: (accessed on 22 March 2021).
25. Ibama Catástrofe Socioambiental Provocada Pelo Rompimento de Barragem da Mineradora Vale em Brumadinho (MG). Available online: (accessed on 22 March 2021).
26. Žibret, G.; Lemiere, B.; Mendez, A.M.; Cormio, C.; Sinnett, D.; Cleall, P.; Szabo, K.; Carvalho, T. National mineral waste databases as an information source for assessing material recovery potential from mine waste, tailings and metallurgical waste. Minerals 2020, 10, 446.
27. Zhu, P.; Xia, B.; Li, H.; Liu, H.; Qian, G. A novel approach to recycle waste serpentine tailing for Mg/Al layered double hydroxide used as adsorption material. Environ. Eng. Sci. 2020, 38, 99–106.
28. Lu, C.; Yang, H.; Wang, J.; Tan, Q.; Fu, L. Utilization of iron tailings to prepare high-surface area mesoporous silica materials. Sci. Total Environ. 2020, 736, 139483.
29. de Magalhães, L.F.; França, S.; dos Santos Oliveira, M.; Peixoto, R.A.F.; Lima Bessa, S.A.; da Silva Bezerra, A.C. Iron ore tailings as a supplementary cementitious material in the production of pigmented cements. J. Clean. Prod. 2020, 274, 123260.
30. Wang, Q.; Li, J.; Zhu, X.; Yao, G.; Wu, P.; Wang, Z.; Lyu, X.; Hu, S.; Qiu, J.; Chen, P.; et al. Approach to the management of gold ore tailings via its application in cement production. J. Clean. Prod. 2020, 269, 122303.

31. Saedi, A.; Jamshidi-Zanjani, A.; Darban, A.K. A review on different methods of activating tailings to improve their cemen titious property as cemented paste and reusability. J. Environ. Manag. 2020, 270, 110881.

32. Gao, S.; Cui, X.; Kang, S.; Ding, Y. Sustainable applications for utilizing molybdenum tailings in concrete. J. Clean. Pro d. 2020, 266, 122020.

33. Tian, X.; Xu, W.; Song, S.; Rao, F.; Xia, L. Effects of curing temperature on the compressive strength and microstructur e of copper tailing-based geopolymers. Chemosphere 2020, 253, 126754.

34. Alfonso, P.; Tomasa, O.; Domenech, L.M.; Garcia-Valles, M.; Martinez, S.; Roca, N. The use of tailings to make glass a s an alternative for sustainable environmental remediation: The case of Osor, Catalonia, Spain. Minerals 2020, 10, 819.

35. Behera, S.K.; Ghosh, C.N.; Mishra, K.; Mishra, D.P.; Singh, P.; Mandal, P.K.; Buragohain, J.; Sethi, M.K. Utilisation of le ad–zinc mill tailings and slag as paste backfill materials. Environ. Earth Sci. 2020, 79, 389.

36. Tsaousi, G.M.; Profitis, L.; Douni, I.; Chatzitheodorides, E.; Panias, D. Development of lightweight insulating building m aterials from perlite wastes. Mater. Constr. 2019, 69, e175.

37. Conde-Vázquez, C.; De Miguel-San Martín, O.; García-Herbosa, G. Artificial arenite from wastes of natural sandstone i ndustry. Mater. Constr. 2019, 69, e178.

38. Gonzalez-Triviño, I.; Pascual-Cosp, J.; Moreno, B.; Benítez-Guerrero, M. Manufacture of ceramics with high mechanica l properties from red mud and granite waste. Mater. Constr. 2019, 69, 1–8.

39. Lemougna, P.N.; Yliniemi, J.; Nguyen, H.; Adesanya, E.; Tanskanen, P.; Kinnunen, P.; Roning, J.; Illikainen, M. Utilisatio n of glass wool waste and mine tailings in high performance building ceramics. J. Build. Eng. 2020, 31, 101383.

40. Chen, Y.; Zhang, Y.; Chen, T.; Zhao, Y.; Bao, S. Preparation of eco-friendly construction bricks from hematite tailings. C onstr. Build. Mater. 2011, 25, 2107–2111.

41. Wang, Y.M. China recycling economy development and its mineral resources' sustainable development. Met. Mine 200 5, 2, 1–3.

42. Ellen MacArthur Foundation. Towards the Circular Economy: Opportunities for the Consumer Goods Sector; Ellen Mac Arthur Foundation: Isle of Wight, UK, 2013; Volume 2.

43. Ellen MacArthur Foundation. Towards the Circular Economy: An Economic and Business Rationale for an Accelerated Transition; Ellen MacArthur Foundation: Isle of Wight, UK, 2013; Volume 1.

44. Sustainable Development Goals. Available online: (accessed on 8 February 2021).

45. Mullite Mineral Data. Available online: (accessed on 8 February 2021).

46. Yan, K.; Guo, Y.; Liu, D.; Ma, Z.; Cheng, F. Thermal decomposition and transformation mechanism of mullite with the ac tion of sodium carbonate. J. Solid State Chem. 2018, 265, 326–331.

47. Schneider, H.; Schreuer, J.; Hildmann, B. Structure and properties of mullite—A review. J. Eur. Ceram. Soc. 2008, 28, 3 29–344.

48. Santos, T.; Hennetier, L.; Costa, V.A.F.; Costa, L.C. Microwave vs conventional porcelain firing: Macroscopic properties. Int. J. Appl. Ceram. Technol. 2020, 17, 2277–2285.

49. Martín-Márquez, J.; Rincón, J.M.; Romero, M. Mullite development on firing in porcelain stoneware bodies. J. Eur. Cera m. Soc. 2010, 30, 1599–1607.

50. Romero, M.; Pérez, J.M. Relation between the microstructure and technological properties of porcelain stoneware. A re view. Mater. Constr. 2015, 65.

51. Cheraitia, A.; Redjimi, Z.; Bououdina, M. Novel mullite-cordierite ceramic refractory fabricated from halloysite and talc. I nt. J. Appl. Ceram. Technol. 2021, 18, 70–80.

52. Halder, K.; Roy, D.; Das, S. A comparative electrical study of nano-crystalline mullite with low dielectric loss due to incor poration of tungsten and molybdenum ion: Their uses in electronic industries. J. Mater. Sci. Mater. Electron. 2015, 26, 5 803–5811.

53. Shibuya, T.; Mizuno, T.; Iuchi, A.; Hasegawa, M. Formation of mullite coating by aerosol deposition and microstructural change after heat exposure. Mater. Trans. 2020, 61, 540–547.

54. Kanwal, S.; Thakare, J.G.; Pandey, C.; Singh, I.; Mahapatra, M.M. Characterization of slurry-based mullite coating dep osited on P91 steel welds. J. Aust. Ceram. Soc. 2019, 55, 519–528.

55. Weinberg, A.V.; Goeuriot, D.; Poirier, J.; Varona, C.; Chaucherie, X. Mullite–zirconia composite for the bonding phase of refractory bricks in hazardous waste incineration rotary kiln. J. Eur. Ceram. Soc. 2021, 41, 995–1002.

56. Chou, Y.S.; Canfield, N.; Bonnett, J.F.; Hardy, J.S.; Stevenson, J.W. Thermal, mechanical, and electrical properties of L SCo/mullite composite contact materials for solid oxide fuel cells. Int. J. Appl. Ceram. Technol. 2020, 17, 2051–2061.

57. Andrade, R.M.; Araújo, A.J.; Alves, H.P.; Grilo, J.P.; Dutra, R.P.; Campos, L.F.; Macedo, D.A. On the physico-mechanica l, electrical and dielectric properties of mullite-glass composites. Ceram. Int. 2019, 45, 18509–18517.

58. Anggono, J. Mullite ceramics: Its properties structure and synthesis. Mullite Ceram. Prop. Struct. Synth. 2005, 7, 1–10.

59. Krenzel, T.F.; Schreuer, J.; Laubner, D.; Cichocki, M.; Schneider, H. Thermo-mechanical properties of mullite ceramics: New data. J. Am. Ceram. Soc. 2019, 102, 416–426.

60. Ilić, S.; Babić, B.; Bjelajac, A.; Stoimenov, N.; Kljajević, L.; Pošarac–Marković, M.; Matović, B. Structural and morpholog ical characterization of iron-doped sol-gel derived mullite powders. Ceram. Int. 2020, 46, 13107–13113.

61. Satoshi, S.; Contreras, C.; Juárez, H.; Aguilera, A.; Serrato, J. Homogeneous precipitation and thermal phase transform ation of mullite ceramic precursor. Int. J. Inorg. Mater. 2001, 3, 625–632.

62. El-Bialy, S.H.; El-Masry, M.A.A.; El-Saeed, M.A.M.; El-Kady, G.M.M. Application of taguchi methodology on the prepara tion of mullite precursor by hydrolysis method. Arab J. Nucl. Sci. Appl. 2017, 50, 131–135.

63. Anggono, J.; Derby, B. Pyrolysis of aluminium loaded polymethylsiloxanes: The influence of Al/PMS ratio on mullite for mation. J. Mater. Sci. 2010, 45, 233–241.

64. Xu, J.P.; Erickson, D.; Roy, S.; Sarin, V. Protective CVD mullite coatings on single-crystal silicon substrates. Jom 2013, 65, 567–573.

65. Hossain, S.K.S.; Pyare, R.; Roy, P.K. Synthesis of in-situ mullite foam using waste rice husk ash derived sol by slip-cas ting route. Ceram. Int. 2020, 46, 10871–10878.

66. Serra, M.F.; Conconi, M.S.; Gauna, M.R.; Suárez, G.; Aglietti, E.F.; Rendtorff, N.M. Mullite (3Al2O3·2SiO2) ceramics ob tained by reaction sintering of rice husk ash and alumina, phase evolution, sintering and microstructure. J. Asian Cera m. Soc. 2016, 4, 61–67.

67. Restrepo, E.; Vargas, F.; López, E.; Baudín, C. The potential of La-containing spent catalysts from fluid catalytic crackin g as feedstock of mullite based refractories. J. Eur. Ceram. Soc. 2020, 40, 6162–6170.

68. Mohammadi, A.; Salehi, E.; Aghazadeh, H.; Ramezani, A.; Eidi, B. An efficient method for recycling spent residue cat-cr acking catalysts (SRC) to prepare broadly-applicable mullite-based wear-resistant ceramics. Appl. Clay Sci. 2020, 187, 105488.

69. Vargas, F.; Restrepo, E.; Rodríguez, J.E.; Vargas, F.; Arbeláez, L.; Caballero, P.; Arias, J.; López, E.; Latorre, G.; Duart e, G. Solid-state synthesis of mullite from spent catalysts for manufacturing refractory brick coatings. Ceram. Int. 2018, 44, 3556–3562.

70. Kongkajun, N.; Cherdhirunkorn, B.; Borwornkiatkaew, W.; Chakartnarodom, P. Utilization of aluminium buffing dust as a raw material for the production of mullite. J. Met. Mater. Miner. 2019, 29, 71–75.

71. Pype, J.; Michielsen, B.; Mullens, S.; Meynen, V. Impact of inorganic waste fines on structure of mullite microspheres b y reaction sintering. J. Eur. Ceram. Soc. 2018, 38, 2612–2620.

72. Khalil, N.M.; Algamal, Y. Recycling of ceramic wastes for the production of high performance mullite refractories. Silicon 2020, 12, 1557–1565.

73. López-Cuevas, J.; Interial-Orejón, E.; Gutiérrez-Chavarría, C.A.; Rendón-Ángeles, J.C. Synthesis and characterization of cordierite, mullite and cordierite-mullite ceramic materials using coal fly ash as raw material. MRS Adv. 2017, 2, 3865 –3872.

74. Yugeswaran, S.; Ananthapadmanabhan, P.V.; Kobayashi, A.; Lusvarghi, L. Transferred arc plasma processed mullite fr om coal ash and bauxite. Ceram. Int. 2011, 37, 3437–3444.

75. Guerreiro, G.G.; Vieira de Andrade, F.; Roberto de Freitas, M. Carbon nanostructures based-adsorbent obtained from ir on ore tailings. Ceram. Int. 2020, 46, 29271–29281.

76. Amaral, I.B.C.; Prat, B.V.; Dos Reis, A.B. Effect of iron mining tailings as a red ceramic additive for decreased sintering temperature. Rev. Mater. 2020, 25, 1.

77. Mendes Protasio, F.N.; Ribeiro de Avillez, R.; Letichevsky, S.; de Andrade Silva, F. The use of iron ore tailings obtained from the Germano dam in the production of a sustainable concrete. J. Clean. Prod. 2021, 278, 123929.

78. do Carmo e Silva Defáveri, K.; dos Santos, L.F.; Franco de Carvalho, J.M.; Peixoto, R.A.F.; Brigolini, G.J. Iron ore tailin g-based geopolymer containing glass wool residue: A study of mechanical and microstructural properties. Constr. Build. Mater. 2019, 220, 375–385.

79. Das, S.K.; Kumar, S.; Ramachandrarao, P. Exploitation of iron ore tailing for the development of ceramic tiles. Waste M anag. 2000, 20, 725–729.

80. Ghosh, I.; Mondal, A.K.; Singh, N.; Das, S.K. Evaluation of iron ore tailings for the production of building materials. Ind. Ceram. 2011, 31, 115–119.

81. Chen, Y.; Zhang, Y.; Chen, T.; Liu, T.; Huang, J. Preparation and characterization of red porcelain tiles with hematite taili ngs. Constr. Build. Mater. 2013, 38, 1083–1088.

82. Fontes, W.C.; Franco de Carvalho, J.M.; Andrade, L.C.R.; Segadães, A.M.; Peixoto, R.A.F. Assessment of the use pote ntial of iron ore tailings in the manufacture of ceramic tiles: From tailings-dams to “brown porcelain”. Constr. Build. Mate r. 2019, 206, 111–121.

83. Peterson, R.; Tabereaux, A. Aluminum production. In Treatise on Process Metallurgy; Elsevier: Stockholm, Sweden, 20 14; pp. 839–917. ISBN 0080969895.

84. Ayres, R.U.; Holmberg, J.; Andersson, B. Materials and the global environment: Waste mining in the 21st century. MRS Bull. 2001, 26, 477–480.

85. Alumina Production Worldwide by Country 2019. Available online: (accessed on 8 February 2021).

86. Khairul, M.A.; Zanganeh, J.; Moghtaderi, B. The composition, recycling and utilisation of Bayer red mud. Resour. Cons erv. Recycl. 2019, 141, 483–498.

87. Yao, L.; Gao, W.; Ma, X.; Fu, H. Properties analysis of asphalt binders containing Bayer red mud. J. Renew. Mater. 202 0, 13, 1122.

88. Zhao, Y.; Chen, P.; Wang, S.; Ji, Y.; Wang, Y.; Wu, B.; Liu, R. Utilization of Bayer red mud derived from bauxite for belite -ferroaluminate cement production. J. Renew. Mater. 2020, 8, 1531–1541.

89. Hu, Y.; Liang, S.; Yang, J.; Chen, Y.; Ye, N.; Ke, Y.; Tao, S.; Xiao, K.; Hu, J.; Hou, H.; et al. Role of Fe species in geopol ymer synthesized from alkali-thermal pretreated Fe-rich Bayer red mud. Constr. Build. Mater. 2019, 200, 398–407.

90. Xu, X.; Song, J.; Li, Y.; Wu, J.; Liu, X.; Zhang, C. The microstructure and properties of ceramic tiles from solid wastes of Bayer red muds. Constr. Build. Mater. 2019, 212, 266–274.

91. Liu, S.; Guan, X.; Zhang, S.; Dou, Z.; Feng, C.; Zhang, H.; Luo, S. Sintered Bayer red mud based ceramic bricks: Micro structure evolution and alkalis immobilization mechanism. Ceram. Int. 2017, 43, 13004–13008.

92. Liu, H.; Qu, Y.; Lu, Y.; Chang, Z.; Yue, Y. Structural, thermal properties and chemical durability of aluminosilicate glasse s prepared by Bayer red mud. Ionics 2017, 23, 2091–2101.

93. Wang, W.; Chen, W.; Liu, H.; Han, C. Recycling of waste red mud for production of ceramic floor tile with high strength and lightweight. J. Alloys Compd. 2018, 748, 876–881.

94. Wang, W.; Chen, W.; Liu, H. Recycling of waste red mud for fabrication of SiC/mullite composite porous ceramics. Cera m. Int. 2019, 45, 9852–9857.

95. da Silva, V.J.; da Silva, M.F.; Gonçalves, W.P.; de Menezes, R.R.; de Araújo Neves, G.; de Lucena Lira, H.; de Lima Sa ntana, L.N. Porous mullite blocks with compositions containing kaolin and alumina waste. Ceram. Int. 2016, 42, 15471– 15478.

96. Global Boron Market Demand by Application in 2014 and 2015. Available online: (accessed on 8 February 2021).

97. Erdogmus, E. Combined effect of waste colemanite and silica fume on properties of cement mortar. Sci. Eng. Compos. Mater. 2014, 21, 369–375.

98. Durgun, M.Y.; Sevinç, A.H. High temperature resistance of concretes with GGBFS, waste glass powder, and colemanit e ore wastes after different cooling conditions. Constr. Build. Mater. 2019, 196, 66–81.

99. Uysal, M.; Al-mashhadani, M.M.; Aygörmez, Y.; Canpolat, O. Effect of using colemanite waste and silica fume as partial replacement on the performance of metakaolin-based geopolymer mortars. Constr. Build. Mater. 2018, 176, 271–282.

100. Kurama, S.; Kara, A.; Kurama, H. The effect of boron waste in phase and microstructural development of a terracotta b ody during firing. J. Eur. Ceram. Soc. 2006, 26, 755–760.

101. Cicek, B.; Karadagli, E.; Duman, F. Valorisation of boron mining wastes in the production of wall and floor tiles. Constr. Build. Mater. 2018, 179, 232–244.

102. Karadagli, E.; Cicek, B. Boron mining and enrichment waste: A promising raw material for porcelain tile production. Int. J. Appl. Ceram. Technol. 2020, 17, 563–572.

103. Mine Production of Molybdenum Worldwide in 2019, by Countries. Available online: (accessed on 2 February 2021).

104. Gao, S.; Zhao, G.; Guo, L.; Zhou, L.; Cui, X.; Yang, H. Mechanical properties of circular thin-tubed molybdenum tailing concrete stubs. Constr. Build. Mater. 2021, 268, 121215.
105. Siddique, S.; Jang, J.G. Assessment of molybdenum mine tailings as filler in cement mortar. J. Build. Eng. 2020, 31, 10 1322.
106. Karhu, M.; Lagerbom, J.; Solismaa, S.; Honkanen, M.; Ismailov, A.; Räisänen, M.L.; Huttunen-Saarivirta, E.; Levänen, E.; Kivikytö-Reponen, P. Mining tailings as raw materials for reaction-sintered aluminosilicate ceramics: Effect of minera logical composition on microstructure and properties. Ceram. Int. 2019, 45, 4840–4848.
107. Major Countries in Worldwide Lithium Mine Production from 2014 to 2019. Available online: (accessed on 8 February 2 021).
108. Projection of Total Worldwide Lithium Supply from 2018 to 2025. Available online: (accessed on 2 August 2020).
109. Salakjani, N.K.; Singh, P.; Nikoloski, A.N. Production of Lithium–A literature review part 1: Pretreatment of spodumene. Miner. Process. Extr. Metall. Rev. 2020, 41, 335–348.
110. Salakjani, N.K.; Singh, P.; Nikoloski, A.N. Production of Lithium—A literature review. Part 2. Extraction from spodumen e. Miner. Process. Extr. Metall. Rev. 2019, 1–16.
111. Rioyo, J.; Tuset, S.; Grau, R. Lithium extraction from spodumene by the traditional sulfuric acid process: A review. Mine r. Process. Extr. Metall. Rev. 2020, 1–10.
112. Lemougna, P.N.; Yliniemi, J.; Ismailov, A.; Levanen, E.; Tanskanen, P.; Kinnunen, P.; Roning, J.; Illikainen, M. Spodume ne tailings for porcelain and structural materials: Effect of temperature (1050-1200 °C) on the sintering and properties. Miner. Eng. 2019, 141, 105843.